



Republic of Iraq  
Ministry of Higher Education  
and Scientific Research  
University of Diyala  
College of Science  
Department of Physics



***Improving the properties of magnetic nano particles (Co-Ni) ferrite by pulsed laser deposition and study its biological effect.***

**A Thesis**  
**Submitted to the Council of the College of Science- University of Diyala in Partial Fulfillment of the Requirements for the Degree of Master of Science in Physics**

**By**

**Marwa Hazem Sabbar**

**B. Sc. in Physics (2019)**

**Supervised By**

**Prof. Dr.  
Tahseen H. Mubarak**

**2022 AD**

**Assist. Prof. Dr.  
Nada S. Ahmed**

**1444AH**

بِسْمِ اللَّهِ الرَّحْمَنِ الرَّحِيمِ  
**(قَالُوا سُبْحَانَكَ لَا عِلْمَ لَنَا**  
**إِلَّا مَا عَلَمْتَنَا إِنَّكَ أَنْتَ**  
**الْعَلِيمُ الْحَكِيمُ ) ٣٢ (**

صدق الله العظيم

سورة البقرة- الآية ٣٢

## *Dedication*

*First of all I thank his Almighty Allah, whose  
Grace enabled me to continue this work and overcome all  
difficulties*

*And*

*To.....*

*My Parents father and mother*

*To.....*

*My brother*

*To.....*

*My friends*

*To.....*

*The people who love and supported me all the time*

## Acknowledgement

First and foremost, I would like to thank Almighty Allah for giving me the strength, knowledge, ability and opportunity to undertake, persevere and complete this research. Without his blessings, this achievement would not have been possible.

There are many people I need to thank for their support and encouragement.

I would like to express my heartfelt thanks to my supervisors, **Prof. Dr. Tahseen H. Mubarak** and **Assist. Prof. Dr. Nada S. Ahmed**, for their guidance, inspiration, and encouragement. I am very grateful for both their expertise and commitments throughout the course of my research.

I express my thanks to head of Physics Department **Asst. Prof. Dr. Ammar A. Habeeb** and all members, especially prof. Dr. Ziad T. Khodiar, Prof. Dr. Nabeel A. Bakr and Prof. Dr. Sabah A. Salman for their cooperation.

It certainly would have been very difficult completing this research without the support from **my parents and my brother**. Their encouragements and supports inspired me to hold out to the end.

I am also grateful to the Physics Department, College of Science at Baghdad University, especially **Dr. Falah A-H.Mutlak** for their kind help during the laboratory work

My thanks and appreciation are to due those who helped me with the words or the work of my professors and brothers students, at the University of Diyala .

## Contents

<i>No.</i>	<i>Subjects</i>	<i>Page No.</i>
	Contents	I
	List of Figures	VI
	List of Tables	IX
	List of Symbols	X
	List of Abbreviations	X
	Abstract	XIII

### Chapter One Introduction and Literature Review

1.1	Introduction	1
1.2	Literature Review	3
1.3	Aim of the Study	9

### Chapter Two Theoretical Part

2.1	Introduction	10
2.2	Ferrite	10
2.3	Spinel ferrites (Cubic ferrites)	11
2.3.1	Normal Spinel	12

2.3.2	Inverse spinel	12
2.3.3	Random spinel	13
2.4	Cobalt Nickle Ferrite structure (Co-Ni FS)	13
2.5	Magnetic metal oxide nanoparticles	14
2.6	Types of Magnetic Materials	16
2.6.1	Diamagnetism	17
2.6.2	Paramagnetic	17
2.6.3	Ferromagnetism	18
2.6.4	Antiferromagnetism	18
2.6.5	Ferrimagnetism	19
2.7	Hysteresis loop and magnetic parameters	20
2.8	Methods of Preparation for Nanoparticles	22
2.8.1	Hydroxides Precipitation	23
2.9	Pulsed Laser Deposition (PLD)	24
2.10	Thermal coefficients	26
2.11	Pressing Process	26
2.12	Sintering	27
2.13	Bacterial Types	28
2.13.1	Escherichia Coli (Gram(-))	28
2.13.2	Staphylococcus bacteria (Gram (+))	28
2.14	Antibacterial activity of Nanoparticles	29
2.15	Structure properties of ferrite	30

2.16	Fourier transform infrared spectroscopy (FTIR)	34
2.17	Filed Emission – Scanning Electron microscopy (FE-SEM)	34
2.18	Magnetic Measurements Techniques	36
2.18.1	Vibrating Sample Magnetometer ( VSM)	36

## Chapter Three

### Experimental Part

3.1	Introduction	38
3.2	Materials	38
3.3	Tools and equipment	39
3.3.1	Mass Measurement Instrument	39
3.3.2	Magnetic Stirrer	39
3.3.3	pH meter	39
3.3.4	Incineration	39
3.4	Preparation of ferrite cobalt nickel( $\text{CO}_{1-x}\text{Ni}_x\text{Fe}_2\text{O}_4$ )	40
3.5	Co-precipitation method to prepare the ferrite-nickel-cobalt $\text{Co}_{1-x}\text{Ni}_x\text{Fe}_2\text{O}_4$	41
3.6	Enhance the characteristic of (Co-Ni) ferrite by laser deposition	44

3.6.1	Powder compaction	44
3.6.2	Pellet formation	44
3.6.3	Pulsed Laser Deposition Technique PLD	45
3.7	Antibacteria test	45
3.7.1	Preparation of Mueller Hinton Agar (MHA)	46
3.7.2	Disc diffusion method	46
3.7.3	Bacterial examine	47
3.8	Device test	48
3.8.1	X-ray Diffraction	48
3.8.2	Field Emission Scanning Electron Microscope	48
3.8.3	Fourier transform infrared spectroscopy (FTIR)	48
3.8.4	Vibrating Sample Magnetometer (VSM)	48

## Chapter Four

### Result and Discussion

4.1	Introduction	49
4.2	Structural Properties	49
4.2.1	XRD for Co-precipitation method	49

4.2.2	XRD for PLD method	54
4.3	Furrier Transform Infra-red spectroscopy	58
4.3.1	FTIR for Co-precipitation method	58
4.3.2	FTIR for PLD method	60
4.4	Field Emission Scanning Electron Microscopy	61
4.4.1	FE-SEM for Co-precipitation method	61
4.4.2	FE-SEM for PLD method	63
4.5	Magnetic Properties	65
4.5.1	VSM for Co-precipitation method	65
4.5.2	VSM for PLD method	67
4.6	Antibacterial activity of $\text{CO}_{1-x}\text{Ni}_x\text{Fe}_2\text{O}_4$	69
4.6.1	Antibacterial activity for Co-precipitation method	70
4.6.2	Antibacterial activity by PLD method	73
4.7	Conclusions	77
4.8	Future Work	78
	References	

## List of Figures

No.	Title	Page No.
2.1	Unit cell of spinel structure $\text{MeFe}_2\text{O}_4$	14
2.2	Periodic table showing different kinds of magnetic materials	16
2.3	(a) The atomic spins of paramagnetic material at a finite temperature, (b) Magnetization change as a function of magnetic field	17
2.4	Parallel alignment of spins in ferromagnetic materials	18
2.5	Antiparallel arrangement of spins in antiferromagnetic lattice	19
2.6	Spin arrangement of ferrimagnetic crystal, A and B are tetrahedral and octahedral respectively	19
2.7	Flow chart of different types of magnetic materials	20
2.8	Hysteresis loop for ferromagnetic materials	21
2.9	Demonstrates a schematic diagram of the PLD technique	25
2.10	shows the powder compaction mechanism	27
2.11	Schematic representation of x-ray diffraction	34
2.12	Constructive interference from the parallel planes	35

2.13	schematic diagram of the operation of the FTIR device	37
2.14	FE-SEM analysis	38
3.3	shows the stages of dissolving solutions	42
3.4	the stage of mixing solutions and obtaining a homogeneous solution	42
3.5	Washing and filtering the powder	43
3.6	Flowchart for the preparation of the compound nickel cobalt	44
3.7	The Transformation of powder to compact sample	45
3.6	experimental setup for laser deposition	46
3.7	Experimental setup for Disc diffusion method	47
3.8	Inhibition zone of bacteria	48
4.1	XRD patterns for $\text{Co}_{1-x}\text{Ni}_x\text{Fe}_2\text{O}_4$ powders prepared at different ratios	51
4.2	Calculation of lattice constant for spinal structure of $\text{Co}_{1-x}\text{Ni}_x\text{Fe}_2\text{O}_4$ powders prepared at different ratios	53
4.3	XRD patterns for $\text{Co}_{1-x}\text{Ni}_x\text{Fe}_2\text{O}_4$ thin films deposited at different ratios	56
4.4	Calculation of lattice constant for spinal structure of $\text{Co}_{1-x}\text{Ni}_x\text{Fe}_2\text{O}_4$ thin films deposited at different ratios	58
4.5	FTIR patterns for $\text{Co}_{1-x}\text{Ni}_x\text{Fe}_2\text{O}_4$ powders at different ratios	60
4.6	FTIR patterns for $\text{Co}_{1-x}\text{Ni}_x\text{Fe}_2\text{O}_4$ thin films at different ratios	61

4.7	FE-SEM images at two magnification powers for $\text{Co}_{1-x}\text{Ni}_x\text{Fe}_2\text{O}_4$ powders prepared at different ratios	63
4.8	FE-SEM images at two magnification powers for $\text{Co}_{1-x}\text{Ni}_x\text{Fe}_2\text{O}_4$ thin films deposited at different ratios	65
4.9	The magneto-hysteresis loop for $\text{Co}_{1-x}\text{Ni}_x\text{Fe}_2\text{O}_4$ powders prepared at different ratios.	66
4.10	variation of residual magnetization and coercive field for $\text{Co}_{1-x}\text{Ni}_x\text{Fe}_2\text{O}_4$ powder at different ratios	67
4.11	The magneto-hysteresis loop for $\text{Co}_{1-x}\text{Ni}_x\text{Fe}_2\text{O}_4$ thin films deposited at different ratios	69
4.12	variation of residual magnetization and coercive field for $\text{Co}_{1-x}\text{Ni}_x\text{Fe}_2\text{O}_4$ thin films at different ratios	70
4.13	Antibacterial activity of $\text{Co}_{1-x}\text{Ni}_x\text{Fe}_2\text{O}_4$ powders at different Ni content against <i>E.Coli</i> . A, control. B, 25%. C, 50%. D, 75%. E, 100%.	72
4.14	Antibacterial activity of $\text{Co}_{1-x}\text{Ni}_x\text{Fe}_2\text{O}_4$ thin films at different Ni content against <i>E.Coli</i> . A, control. B, 25%. C, 50%. D, 75%. E, 100%.	73
4.15	Antibacterial activity of $\text{Co}_{1-x}\text{Ni}_x\text{Fe}_2\text{O}_4$ powders at different Ni content against <i>S. aureus</i> . A, control. B, 25%. C, 50%. D, 75%. E, 100%.	75
4.16	Antibacterial activity of $\text{Co}_{1-x}\text{Ni}_x\text{Fe}_2\text{O}_4$ thin films at different Ni content against <i>S. aureus</i> . A, control. B, 25%. C, 50%. D, 75%. E, 100%	76

## List of Tables

No.	Title	Page No.
3.1	Chemicals Used	40
4.1	XRD parameters for $\text{Co}_{1-x}\text{Ni}_x\text{Fe}_2\text{O}_4$ powders prepared at different ratios.	52
4.2	lattice constant (a), lattice volume (V), lattice density ( $\rho_x$ ), and ion jump lengths ( $L_A$ , $L_B$ ) for $\text{Co}_{1-x}\text{Ni}_x\text{Fe}_2\text{O}_4$ powders prepared at different ratios	55
4.3	XRD parameters for $\text{Co}_{1-x}\text{Ni}_x\text{Fe}_2\text{O}_4$ thin films prepared at different ratios	57
4.4	lattice constant (a), lattice volume (V), lattice density ( $\rho_x$ ), and ion jump lengths ( $L_A$ , $L_B$ ) for $\text{Co}_{1-x}\text{Ni}_x\text{Fe}_2\text{O}_4$ thin films prepared at different ratios.	59
4.5	FTIR bands for $\text{Co}_{1-x}\text{Ni}_x\text{Fe}_2\text{O}_4$ powders at different ratios.	60
4.6	FTIR bands for $\text{Co}_{1-x}\text{Ni}_x\text{Fe}_2\text{O}_4$ thin films at different ratios	62
4.7	Magnetization parameters for $\text{Co}_{1-x}\text{Ni}_x\text{Fe}_2\text{O}_4$ powder at different ratios	67
4.8	Magnetization parameters for $\text{Co}_{1-x}\text{Ni}_x\text{Fe}_2\text{O}_4$ thin films at different ratios	69

## ***List of symbols***

Symbols	Description	Units
$d_{hkl}$	Inter-atomic distances	nm
$hkl$	Miller indices	nm
D	Crystalline size	nm
h	Planck constant	J/s
$\Theta$	Diffraction angle	Degree
$\lambda$	Wavelength	nm

## **List of Abbreviations**

Abbreviations	Definition
NPs	Nanoparticles
XRD	X-ray diffraction
FWHM	Full width at half maximum
TEM	Transmission electron microscopy
FT-IR	Fourier transform infrared spectroscopy
SEM	Scanning electron microscopy
FE-SEM	Field emission-scanning electron microscopes

VSM	Vibrating sample magnetometer
MRI	Magnetic resonance imaging
FWHM	Full width at half-maximum
PXRD	Powder X-ray diffraction
GMR	Giant magneto resistance
PLD	Pulse Laser Depostion
MHA	Mueller Hinton Agar
RFA	Radio frequency ablation
MNPs	Micronized nanoparticals
MR	Magmatic Recording
MMONPs	magnetic metal oxide nanoparticles

## **ABSTRACT:**

In this research, we prepared magnetic nano particles in format  $\text{Co}_{1-x}\text{Ni}_x\text{Fe}_2\text{O}_4$  in two methods. The first method is Co-precipitationnand were used pulsed laser deposition (PLD).

We used a mixture of nickel nitrate, cobalt nitrate, iron nitrate, as well as sodium hydroxide as a chelating agent to balance the ratio of the oxidizing agent.

The ferrite NPs were calcined at temperatures (300 °C) for 3 hr. to remove water content and unwanted impurities and to obtain a better single-phase spinel structure. The resulting powder is then compressed into a disc with a diameter of (2 cm) and then we use laser deposition technology to obtain thin film.

Structure and magnetic properties of the NPs were tested using XRD, FE-SEM, FTIR, and finally the Vibrating Sample Magnetometer (VSM), which revealed the presence of Super para magnetic samples. The x-ray spectrum shows that the pattern of the particles formed is of the face -centered cubic and the theoretical values of the lattice constant and crystalline size (D) were calculated .The crystalline size calculated was located in the range (22.6-26.6 nm), either in the pulsed laser deposition method in the range (13.7)nm, which reflects the highly crystalline nature of these nanoparticles. The FTIR spectrum shows two absorption bands ranging between 400 and 600  $\text{cm}^{-1}$ . These bands indicated that the composition of the spectrum for all the samples is ferrite.

The Field emission scanning electron microscopes (FE-SEM) images confirmed that the preparation methods produced spherical nanoparticles with a slight change in the particle size distribution. The average particle size by co-precipitation had estimated to be about 23 nm and the average particle size by pulsed laser deposition(PLD) method had estimated to be about 20 nm.

The magnetic properties vibrating sample magnetometer (VSM) showed good correlation with the structural parameters of the spinal structure, which increased with the Ni content.

When using nanoparticles prepared by co-precipitation method on *Escherichia coli* and *Streptococcus* bacteria, the highest inhibition zone ranged from (27-33) mm. When using nanoparticles prepared by using the method of pulsed laser deposition on the same types of bacteria, (*S.aureus*) was found to have the highest inhibition zone (22-32) mm , while Bacteria(*Escherichia coli*) the inhibition zone ( 27-30) mm.

# Chapter One

Introduction

And

Literature Review

## 1.1 Introduction

A horizontal sequence of 15 empty square boxes arranged in three rows of five. The boxes are evenly spaced and aligned horizontally.

A horizontal sequence of 24 empty square boxes arranged in three rows of 8. The boxes are evenly spaced and aligned horizontally.

The image consists of five vertical columns of empty boxes. Each column contains two rows of boxes. The first three columns have 5 boxes per row, while the last two columns have 6 boxes per row. This creates a visual pattern of increasing box counts from left to right.

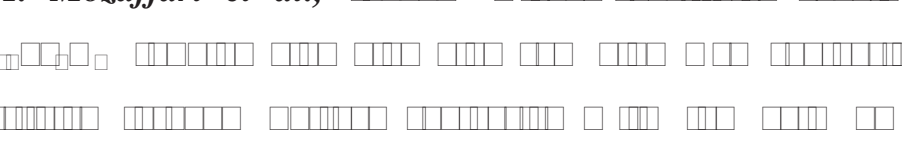
properties, ferrites can be categorized as “soft” and “hard” ferrite. Soft

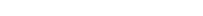
properties, ferrites can be categorized as “soft” and “hard” ferrite. Soft

properties, ferrites can be categorized as “soft” and “hard” ferrite. Soft

The image consists of ten identical horizontal rows, each containing ten empty square boxes arranged in a single row. These boxes are intended for users to draw tally marks (such as vertical strokes or short lines) to keep track of counts for different categories.

## 1.2. Literature Review

*M. Mozaffari et al.*, 

*Muhammad et al.*,     
         
         
         
         
         
         
         
         
       

*Zalite et al.*,   
  
  
  
  
  
  
  
  


The figure consists of nine horizontal rows of binary digits (0s and 1s) arranged vertically. Each row represents a sequence of DNA. The digits are represented by small squares: black for 1 and white for 0. In the fifth row from the top, there is a label '1-x' positioned to the left of a specific sequence of digits. The sequences vary in length and pattern across the rows.

*Suresh Sagadevan et al.,* സുരേഷ് സഗദേവൻ എന്നാർത്ഥിയാണ്

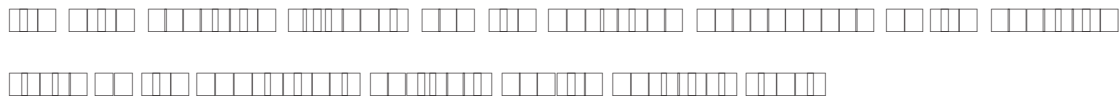
സുരേഷ് സഗദേവൻ എന്ന പേരിൽ അറിയപ്പെടുന്ന ഒരു മലബാറിയാണ്. കൊച്ചിയിൽ ജീവിച്ചു വരുന്ന ഒരു മലബാറിയാണ്. സുരേഷ് സഗദേവൻ എന്ന പേരിൽ അറിയപ്പെടുന്ന ഒരു മലബാറിയാണ്. കൊച്ചിയിൽ ജീവിച്ചു വരുന്ന ഒരു മലബാറിയാണ്.

*Muhammad Arshad et al., (۲۰۱۷)* മുഹമ്മദ് അർഷദ് എന്നാർത്ഥിയാണ്

മുഹമ്മദ് അർഷദ് എന്ന പേരിൽ അറിയപ്പെടുന്ന ഒരു മലബാറിയാണ്. കൊച്ചിയിൽ ജീവിച്ചു വരുന്ന ഒരു മലബാറിയാണ്. മുഹമ്മദ് അർഷദ് എന്ന പേരിൽ അറിയപ്പെടുന്ന ഒരു മലബാറിയാണ്. കൊച്ചിയിൽ ജീവിച്ചു വരുന്ന ഒരു മലബാറിയാണ്.

*Mikio Kishimoto et al., (۲۰۱۷)* മികോ കിഷിമോ എന്നാർത്ഥിയാണ്

മികോ കിഷിമോ എന്ന പേരിൽ അറിയപ്പെടുന്ന ഒരു മലബാറിയാണ്. കൊച്ചിയിൽ ജീവിച്ചു വരുന്ന ഒരു മലബാറിയാണ്. മികോ കിഷിമോ എന്ന പേരിൽ അറിയപ്പെടുന്ന ഒരു മലബാറിയാണ്. കൊച്ചിയിൽ ജീവിച്ചു വരുന്ന ഒരു മലബാറിയാണ്.



**S. V. Bhandare et al.**, (2020) Studied changes in spinel ferrites structural and magnetic properties by doping. Magnesium the cation that occupies the tetrahedral position, rather than nickel, occupies. He created nanocrystals at octahedral sites in Co-Ni Ferrite ( $\text{Co}_{0.5}\text{Ni}_{0.5}\text{Fe}_2\text{O}_4$ ) ceramics, where he created nanocrystals. Sol-gel  $\text{Co}_{0.5}\text{Mg}_x\text{Ni}_{0.5-x}\text{Fe}_2\text{O}_4$  Ceramic Powder Samples ( $x = 0, 0.1, 0.2, 0.3, 0.4$ ) The spontaneous combustion method was followed by sintering at 600 °C in air for two hours. X-ray diffraction The XRD patterns of the composite samples confirm the single-phase crystalline spinel structure with Cubic symmetry. Crystal sizes were found for all samples.be in the range of 30–38 nm. Scanning electron micrographs FTIR spectra confirm the formation of the spinel phase. Through the observed vibrational bands assigned to tetrahedral ( $T_d$ ) and octahedral (OH), interstitial complexes in the spinel structure. Magnetic measurements indicate low Saturation magnetization ( $M_s$ ) with increasing Mg concentration [22].

**Sabah M. Ali Ridha et al.**, (2021) Studied Preparing nickel-saturated ferrite nanoparticles (NPs) with the chemical formula  $\text{Co}_{1-x}\text{Ni}_x\text{Fe}_2\text{O}_4$  (where,  $x = 0, 0.5$ , and  $1$ ) using the sol-gel method at low temperature (200 °C). To balance the oxidizing agent, citric acid was used as a chelating agent with a mixture of nickel nitrate and ferric nitrate solutions in a 3:1 ratio .The resulting ferrite NPs were calcined at various temperatures (200, 400, 600, and 800 °C) for 4 h in the air to remove water content and unwanted impurities and to obtain a better structure than the single-phase spinel. X-ray analysis (XRD). XRD analysis shows the structure of a single-phase spinel at the nanoscale. The crystal size calculated from the FWHM of the strongest peak (311) lies in the range

(20-44 nm) for  $\text{Co}_{1-x}\text{Ni}_x\text{Fe}_2\text{O}_4$  ferrite NPs. Because  $\text{Co}_{0.5}\text{Ni}_{0.5}\text{Fe}_2\text{O}_4$  NPs have a larger crystal size than  $\text{NiFe}_2\text{O}_4$  but smaller than  $\text{CoFe}_2\text{O}_4$  NPs. SEM images show spherical and homogeneous NPs. The particle size morphology ranges from 25-40 nm, reflecting the highly crystalline nature of these nanoparticles [23].

**Durgadossi S.U et al.**, (2021) Synthesized the Nickel ferrite by co-precipitation. X-ray diffraction pattern confirms the formation of cubic spinel structure with lattice constant 8.34 Å. Structural properties like X-ray density, average crystalline size, bond length, dislocation density, and microstrain have been studied. The scanning electron microscope images show the grain of bead structures. The Fourier transform infrared spectroscopy spectrum of nickel ferrite under investigation reveals the formation of a cubic spinel structure showing two significant absorption bands, corresponding to high-frequency band  $v_1$  and low-frequency band  $v_2$  arising from tetrahedral (□) and octahedral (□) interstitial sites respectively [24].

### 1.3 Aim of the Present Work

1. preparation Co-Ni ferrite nano particles by simple and very fast methods.
2. Studying the structural properties of XRD,FTIR,F<sub>□</sub>-S<sub>□</sub>M and the magnetic properties □SM of the prepared particles
3. Improving the properties of the prepared nickel cobalt using pulsed laser deposition
4. Testing the effectiveness of nano-ferrite as anti-bacterials against two types of □ram-positive and □ram-negative bacteria